Journal Homepage: - www.journalijar.com

INTERNATIONAL JOURNAL OF ADVANCED RESEARCH (IJAR)

Article DOI: 10.21474/IJAR01/23463
DOI URL: http://dx.doi.org/10.21474/IJAR01/23463

ISSN (O): 2320-5407
ISSN (P): 3107-4928

RESEARCH ARTICLE

PETROGRAPHIC AND MINERALOGICAL CHARACTERIZATION OF GRANITOIDS AND PEGMATITES IN THE PAN-AFRICAN MASSIF OF HARAZE DJOMBO (BATHA, CENTRAL CHAD)

MEBAH Tapsala[1], LIKIUS Andossa[1,4], Rigobert Tchameni[2] and HAR Nicolae[3]

1. Department of Geology, Faculty of Exact and Applied Sciences, University of N'Djamena, Chad.
2. Department of Earth Sciences, Faculty of Sciences, University of Ngaoundéré, Cameroon .
3. Department of Geology, Babeș-Bolyai University, Cluj-Napoca, Romania .
4. Department of Paleontology, Faculty of Exact and Applied Sciences, University of N'Djamena, Chad.

Manuscript Info

Manuscript History
Received: 10 March 2026
Final Accepted: 12 April 2026
Published: May 2026

Key words:-
Chad, Batha Massif, Pan-African, Post-collisional granite, X-ray diffraction (XRD), Saharan Metacraton.

Abstract

The Batha Massif, located in central Chad, occupies a key position at the transition between the Saharan Metacraton and the Central African Pan-African belt. The geodynamic evolution and metallogenic potential of this area remain poorly constrained due to the scarcity of modern analytical data. This study aims to characterize the mineralized granitoi ds and pegmatites of the Djombo and Gleb mounts (Haraze Djombo Department) through an approach combining field prospecting, optical petrography, and powder X-ray diffraction (XRD). Observations reveal two post-collisional magmatic facies emplaced during crustal relaxation (~570-560 Ma): a peraluminous biotite-muscovite granite (Djombo) and a calc-alkaline amphibole-biotite granite (Gleb). XRD analysis of the Djombo granite confirms a differentiated felsic assemblage (quartz, microcline, albite) and reveals the presence of secondary tremolite. The unprecedented identification of this amphibole indicates intense hydrot hermal alteration in greenschist facies, demonstrating that the southern margin of the Saharan Metacraton corresponded to a reactivated and fractured margin that drained deep fluids. Furthermore, analysis of Gleb veins reveals a single-phase signature of exceptionally pure quartz (>95%) coupled with spectacular cataclastic texture. The conjunction of allanite-bearing fertile granites, marked hydrothermal alteration (tremolite), and injection of pure siliceous fluids into active shear zones constitutes the classic signature of orogenic gold mineralization, thus scientifically validating the strong regional economic potential.

Introduction:-

In Chad, the Precambrian basement crops out in the massifs of Tibesti (North), Ouaddaï (East), Guéra (Center), Yadé, and Mayo-Kebbi (West), the latter belonging to the Central African Pan-African belt (Fig. 1a). These formations cover 15-20% of the territory, the remainder consisting of Phanerozoic sedimentary formations. Most

Corresponding Author:- MEBAH Tapsala
Address:- Department of Geology, Faculty of Exact and Applied Sciences, University of N'Djamena, Chad.

studies (Abdelsalam et *al.,* 2002; Liégeois et *al.,* 2013; Shellnutt et *al.,* 2017) place these regions within the Saharan Metacraton, a vast continental domain of 5,000,000 km² extending from the Arabian-Nubian Shield to the Tuareg Shield and from the Mediterranean to the Congo Craton (Fig. 1b). The Guéra Massif, in the center of the country, consists essentially of heterogeneous Ediacaran granitoids (570-560 Ma) interpreted as post-collisional, emplaced during crustal relaxation following the Saharan Metacraton – Congo Craton collision (610-590 Ma). Inherited zircons (~1.0 Ga and ~1.9 Ga) attest to a contribution from ancient basement (Shellnutt et al., 2017, 2020; Blades et *al.,* 2021). However, previous studies, mostly limited to petrographic descriptions (Vincent, 1956; Kasser, 1995), have not constrained the geodynamic evolution or the origin of mineralized occurrences (gold, graphite, iron) identified in the region. This study aims to characterize the mineralized granites and pegmatites of the Djombo and Gleb mounts (Haraze Djombo Department, Batha region) through a petrographic and mineralogical (XRD) approach in order to: (i) define their mineralogical assemblage and emplacement context; (ii) constrain the applicable geodynamic model; (iii) assess the regional metallogenic potential.

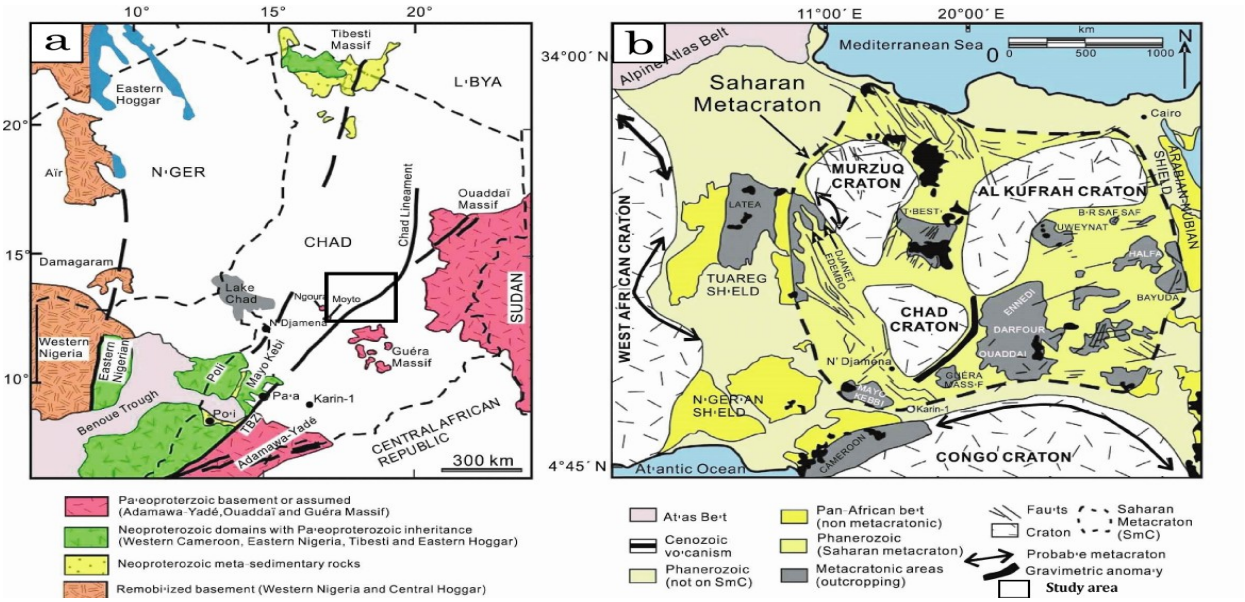

Figure 1.Different geological correlations of the southern boundary of the Saharan Metacraton. (a) Correlation of Central African rock units as interpreted by Penaye et al. (2006). (b) Boundary of the Saharan Metacraton as delineated by Abdelsalam et al., (2002) and Liégeois et al., (2013).

Materials and Methods:-

Sampling and fieldwork

Sampling was conducted on the Djombo and Gleb mounts (Batha), a sector extracted from the geological map of Chad (Kasser, 1995). In situ exploration (compass, GPS, hammer) enabled identification and photographing of major facies. Twelve (12) representative samples were collected and coded: DJ (Djombo granite), GL (Gleb granite), and PGL (pegmatites/quartz veins). The spatial distribution of these sampling points is illustrated in Figure 2.

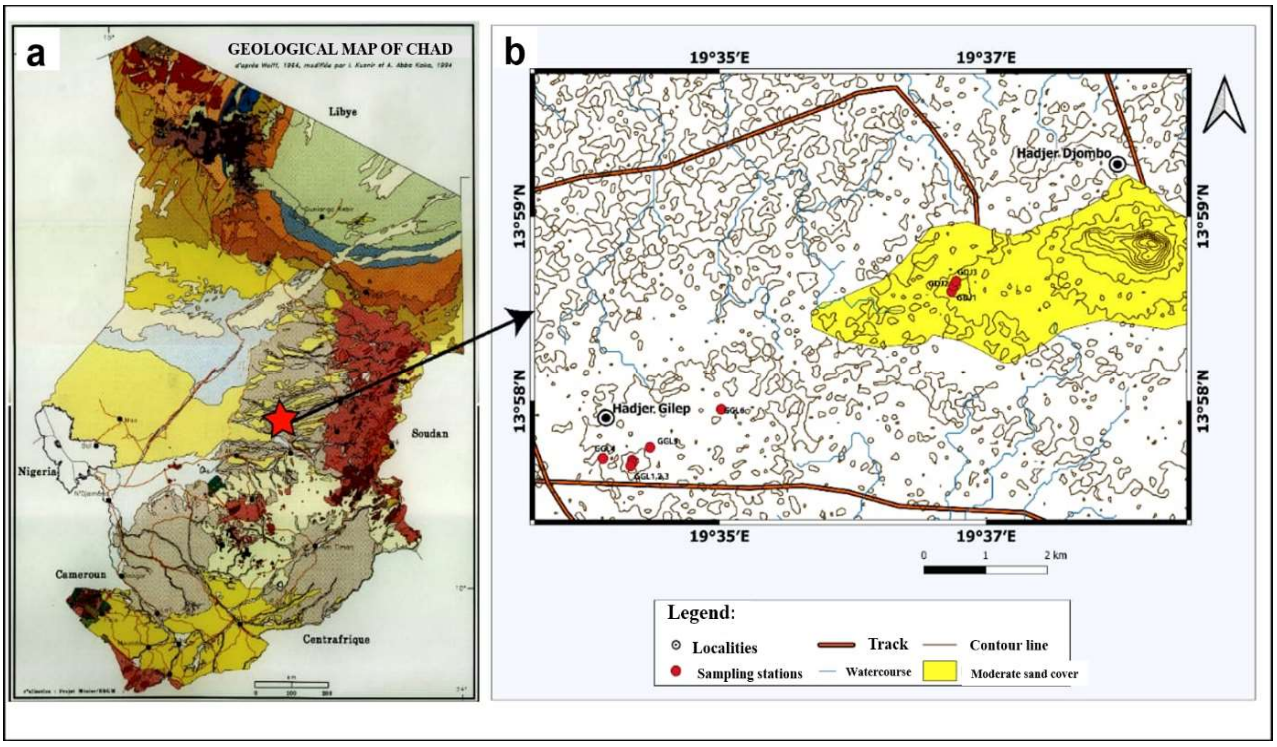

Figure 2.Location and geological map of the study area. (a) Situation of the Haraze Djombo massif in the geological context of central Chad; (b) Detailed geological map of the Djombo and Gleb mounts (extracted and adapted from Kasser, 1995) showing the spatial distribution of sampling stations. DJ: Djombo granites; GL: Gleb granites; PGL: Gleb pegmatites and quartz veins.

Petrography

Selected samples were prepared as polished thin sections (standard thickness of 30 µm). Observation of textures and mineralogical assemblages was performed at the Geology Laboratory of Babeş-Bolyai University (Cluj-Napoca, Romania) using a Nikon Optiphot T2-Pol polarizing microscope in plane-polarized light (PPL) and cross-polarized light (XPL).

X-ray diffraction (XRD)

Mineralogical analysis by XRD was performed on powder at the Geology Department of Babeş-Bolyai University (Romania). Samples were finely ground (<10 µm) using an agate mortar and then analyzed using a Bruker D8 Advance diffractometer equipped with a Cu Kα source (λ = 1.54060 Å), an Fe filter (0.01 mm), and a one-dimensional LynxEye detector. Operating parameters were: 40 kV, 40 mA, scanning from 5° to 65° (2θ) with a step size of 0.02° and a counting time of 0.2 s/step. Identification of mineral phases was performed using Diffrac.Suite EVA software and the PDF2 database (version 2.1202) from the ICDD (International Centre for Diffraction Data).

Results:-

Macroscopic and microscopic description

Lithology and Petrography

The Djombo and Gleb mounts, approximately 8 km apart (Fig. 3a-b), form prominent granitic reliefs dominating a vast alluvial plain. This sector is currently subject to intense gold prospecting activities due to the presence of mineralized structures. Rock outcrops mainly expose pink granites with coarse-grained texture, partially masked by wind-blown sand cover.

Figure 3.Macroscopic facies of the Gleb and Djombo Mounts. a-b: Outcrop and rock blocks on the Gleb and Djombo Mounts.

Amphibole-biotite granite (Gleb Mount)

The amphibole-biotite granite is characterized by medium grain size and a mesocratic tendency, related to biotite enrichment at the expense of K-feldspar. Some blocks are superficially marked by alteration giving a pink color to the rock (Fig. 4a). On fresh fracture surfaces, the whitish facies speckled with black allows clear distinction of quartz, feldspars, and biotite (Fig. 4b). Polarizing microscope observation reveals a heterogranular granular texture. Plagioclases undergo intense saussuritization, highlighted by sericite-clay felting that masks twin planes, while quartz exhibits clear microfracturing (Fig. 4c-d). Mafic minerals form synneusis aggregates where prismatic green hornblende and yellow-brown biotite undergoing chloritization coexist (Fig. 4e-f). Euhedral allanite (up to 0.45 mm) is very abundant and spatially associated with opaque minerals. The mineralogical assemblage is complemented by apatite, zircon, granular epidote, and secondary calcite (Fig. 4g-h). Microstructurally, myrmekites characteristically develop at plagioclase margins, at the interface with perthitic orthoclase crystals (Fig. 4i-j).

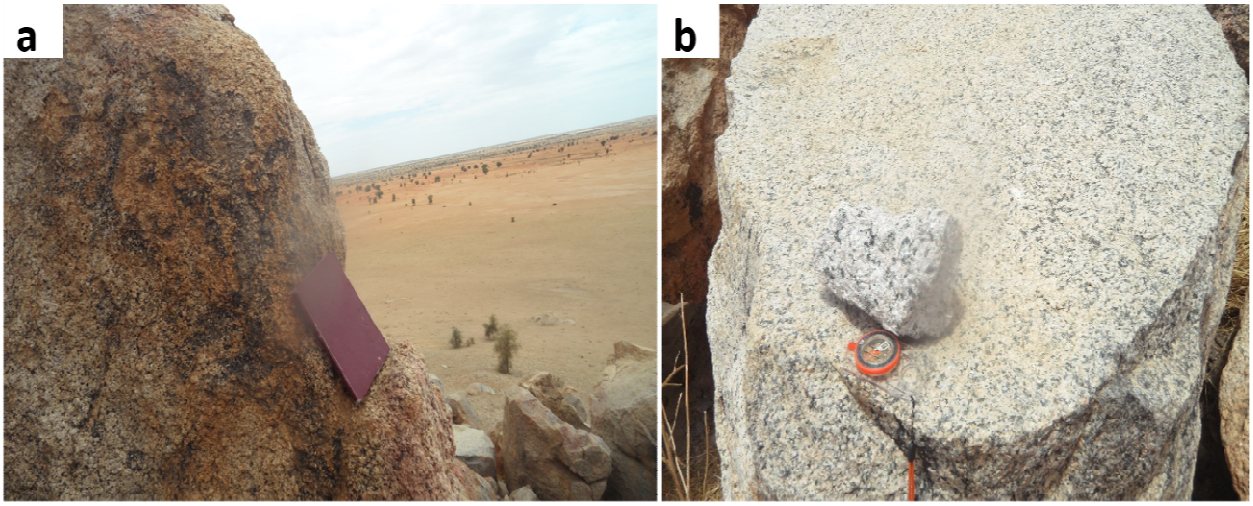

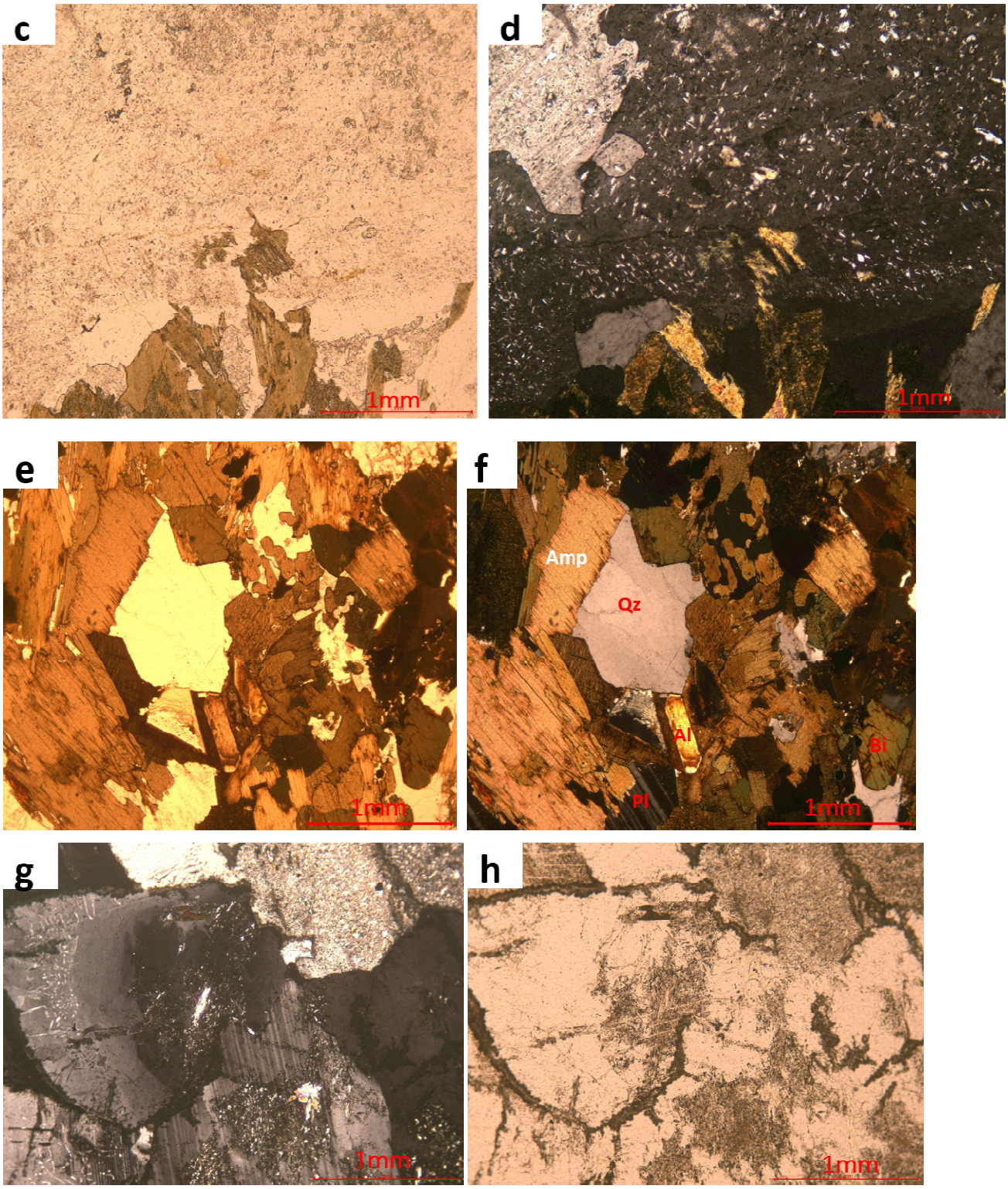

Figure 4.Macroscopic and microscopic characterization of amphibole-biotite granite. a-b: Mesocratic macroscopic appearance on fresh fracture. c-d: Intensely saussuritized plagioclase masking twins. e-f: Mafic aggregate of green hornblende and chloritized biotite. g-h: Development of myrmekites at plagioclase margins.

Biotite-muscovite granite (Djombo Mount)

Biotite granites crop out as chaotic blocks on Djombo Mount and display a coarse-grained texture on fresh fracture surfaces (Fig. 5a-b). Under the microscope, it exhibits a granular texture with porphyritic tendency (Fig. 5c). Subhedral plagioclase (1.4 mm) and enclosing microcline are molded by large patches of quartz with undulatory extinction (Fig. 5d). The petrographic peculiarity of this facies lies in the association of large brown chloritized biotite laths (rich in metamict zircons) with primary muscovite in clear flakes, attesting to differentiated peraluminous magmatism. Prismatic zoned allanite (up to 1.4 mm), yellow-brown titanite, and magnetite constitute the accessory assemblage (Fig. 5e).

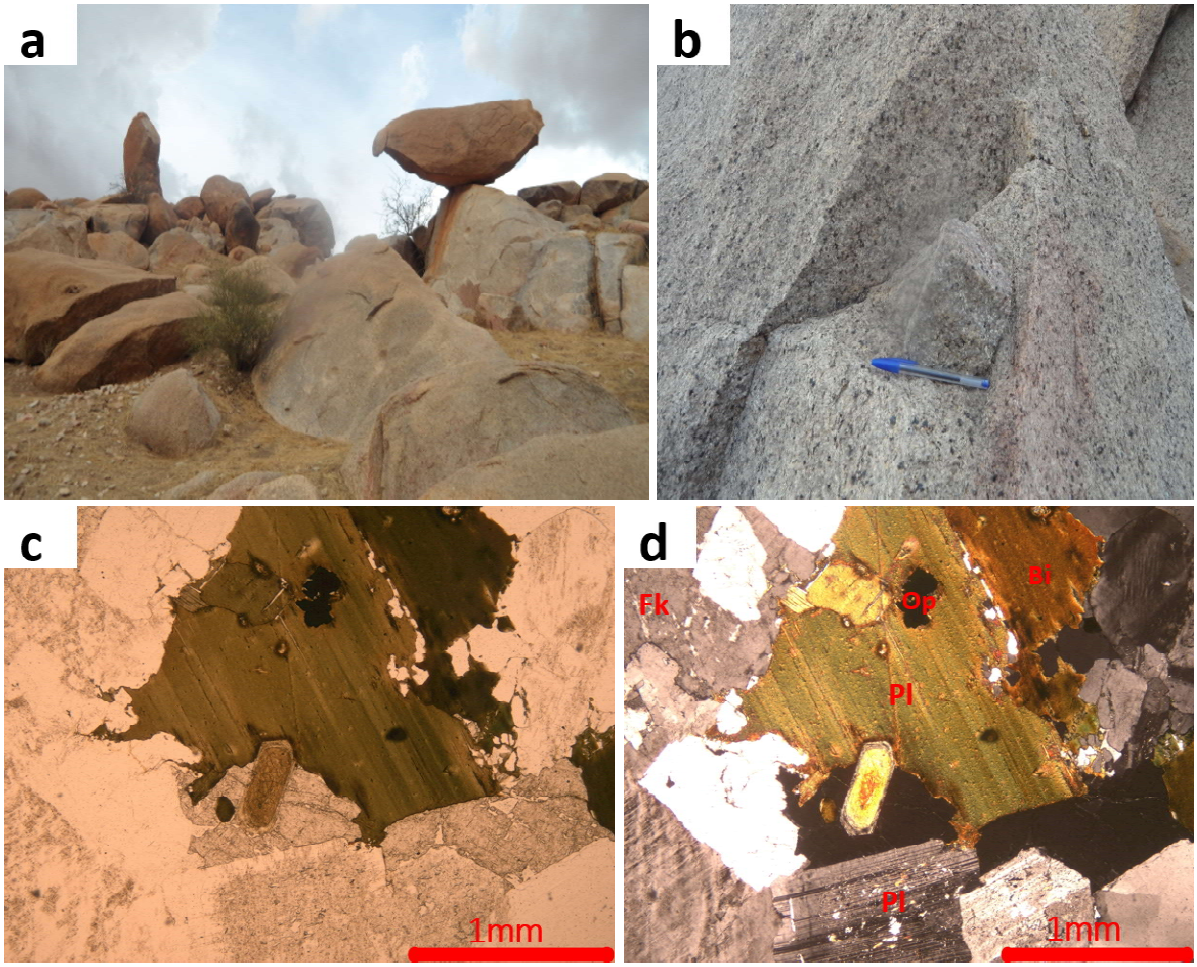

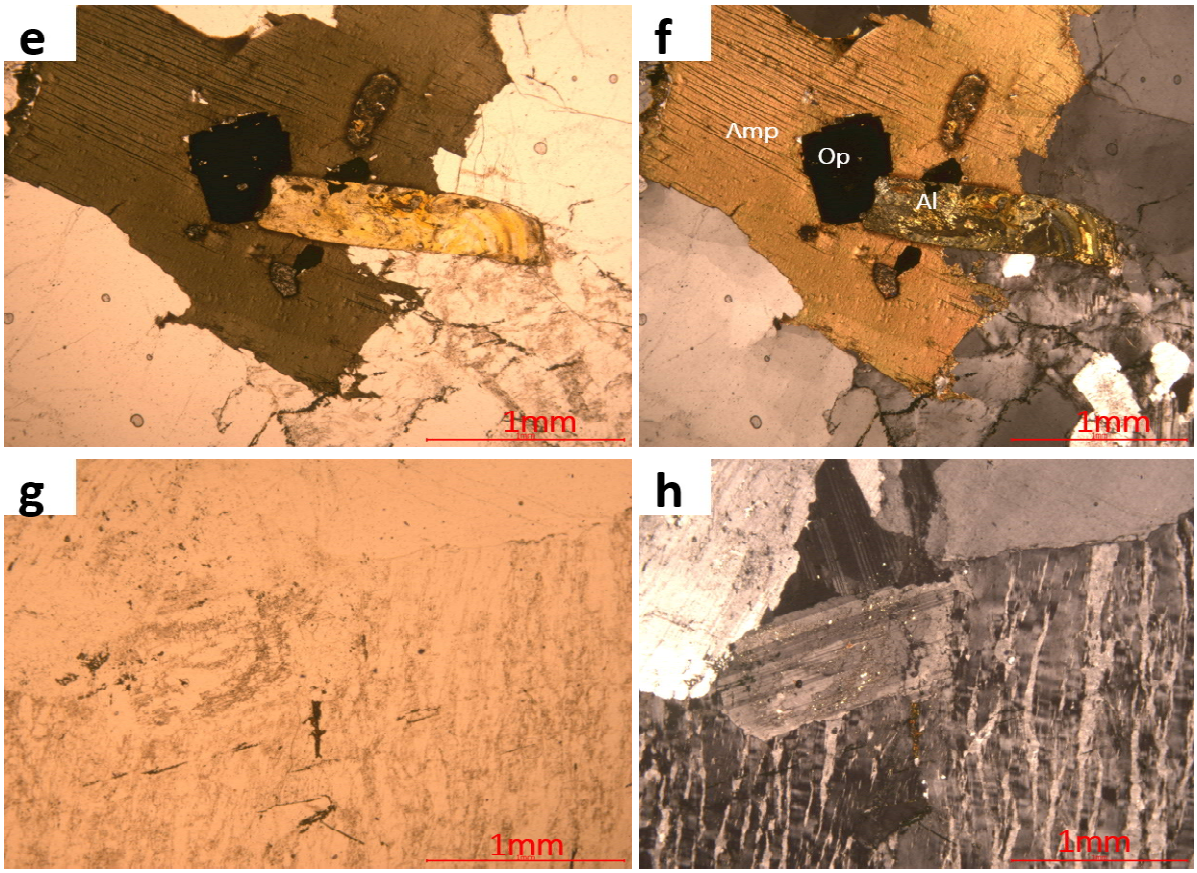

Figure 5.Biotite-muscovite granite from Djombo (sample DJ). a-b: Fresh fracture with coarse-grained texture. c: Granular porphyritic texture (XPL). d: Plagioclase, microcline, and quartz with undulatory extinction (XPL). e: Primary biotite-muscovite association and accessory minerals: zoned allanite, titanite, magnetite (XPL/PPL).

Pegmatites and quartz veins (Gleb sector)

Pegmatites and massive milky quartz veins frequently appear at the summit of the mounts and in drill cores, intimately linked to gold mineralization (Fig. 6a-b). Pegmatites are frequently more or less altered at the surface and at depth in gold exploration drill holes, associated with quartz crystals (Fig. 6c-d). Observations on contacts between granites and host rocks are quite sharp. Microscopic examination of the pegmatite reveals a spectacular cataclastic texture (Fig. 6e). Large angular sharp-edged quartz porphyroclasts (up to 3.3 mm) are dispersed in a finely crushed dark matrix. The dense network of anastomosing microfractures fragmenting the crystals is highlighted by iron oxide deposits and hydrothermal cements, witnesses of major brittle fracturing (Fig. 6f).

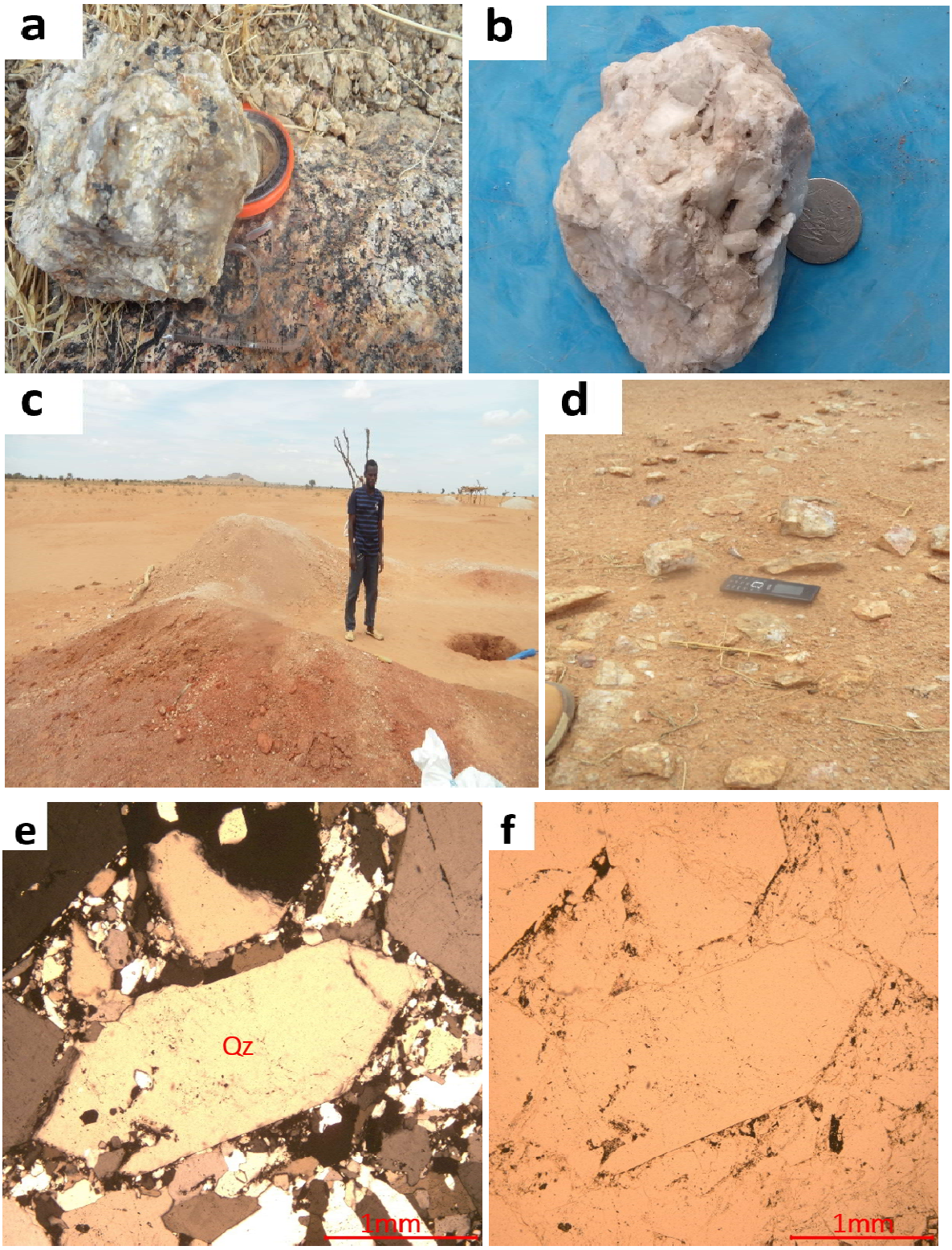

Figure 6.Pegmatites and quartz veins from the Gleb sector. a: Mineralized pegmatite outcrop. b: Massive milky quartz vein. c: Cataclastic texture with angular porphyroclasts (XPL). d-e: Cataclastic texture and anastomosing microfractures filled with iron oxides.

Mineralogical characterization by XRD

Amphibole-biotite granite from Djombo (Sample DDJ)

The X-ray diffraction pattern (Fig. 7) of sample DDJ, acquired in coupled θ–2θ geometry with Cu Kα radiation (λ = 1.54060 Å), reveals a polyphase mineralogical assemblage with crystalline dominance. The obtained spectrum shows a succession of sharp and well-defined peaks, indicating the presence of crystalline phases. Major peaks are located mainly at positions 20.8°, 26.6°, 27.5°, 29.4°, 40.2°, and 50.1° in 2θ, with variable intensities reaching approximately 2900 counts. The spectrum shows a series of variable intensity peaks distributed between 5° and 65° 2θ, indicating the presence of well-developed crystalline phases. The reduced width of the peaks suggests well-ordered crystals.

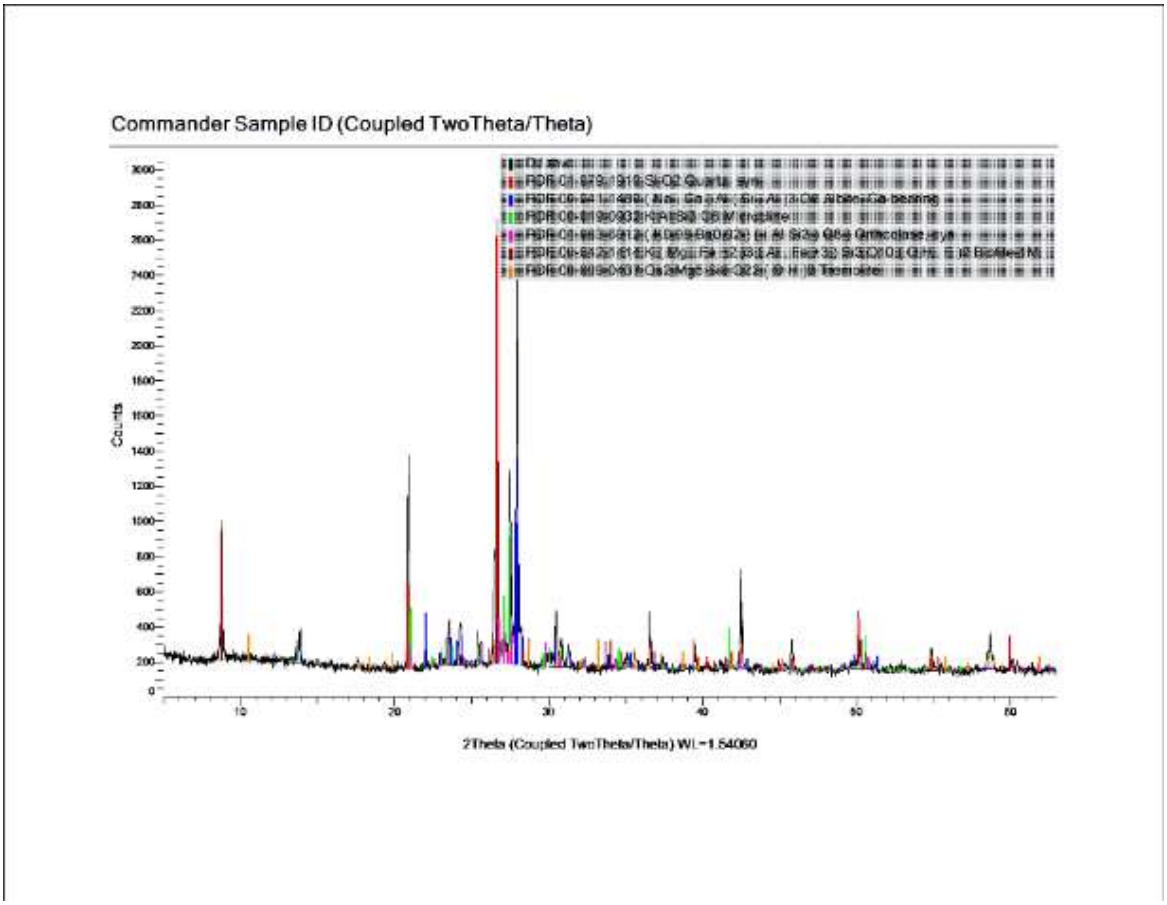

Figure 7:X-ray diffraction (XRD) spectrum of the Djombo sample, showing reflections of quartz, albite, orthoclase, biotite, and tremolite.

The most intense reflection of the diffractogram is located at 2θ ≈ 26.6°, a characteristic position of the main quartz (SiO_2) line. The marked intensity of this peak indicates that quartz constitutes one of the main phases of the sample (Fig. 8). This identification is corroborated by the presence of several secondary reflections observed notably around 20.8°, 36.5°, 39.5–40°, 42.5°, 50.1°, and 59.9° (2θ), in accordance with reference file PDF 01-079-1910. The sharpness of these peaks indicates a well-ordered structure of the quartz phase, although this does not appear to be the only component of the mineral assemblage.

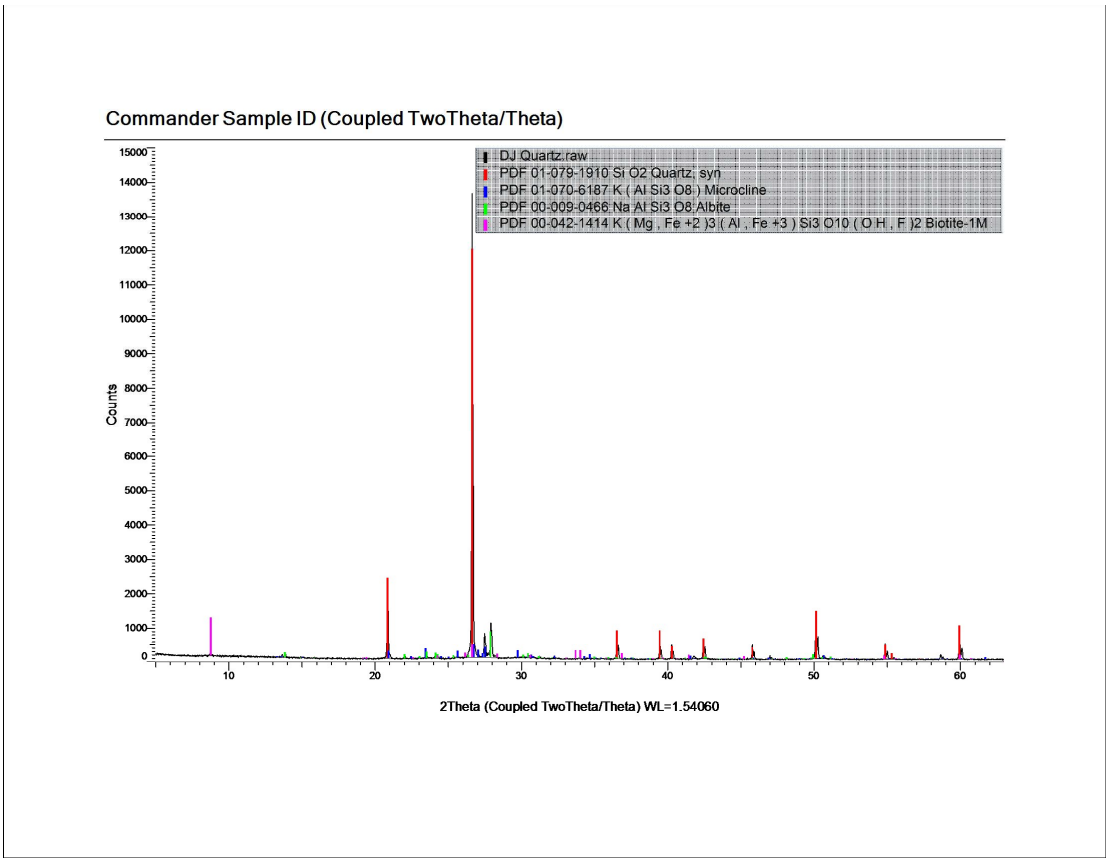

Figure 8:X-ray diffraction (XRD) spectrum of the Djombo sample, showing quartz reflections.

The feldspar reflection pattern is manifested by the presence of calcic albite [(Na,Ca)Al(Si,Al)$_3$O$_8$], identified from reference file PDF 00-041-1480, suggested by several low to medium intensity reflections, mainly concentrated in the ranges of 22–30° and 40–50° (2θ) (Fig. 9). This phase indicates the presence of a sodic-calcic plagioclase in the sample. The diagram also indicates the presence of microcline (KAlSi$_3$O$_8$), referenced in file PDF 00-019-0932, several lines of which are observed in the intervals 20–23° and 27–30° (2θ). This K-feldspar contributes significantly to the complexity of the intermediate angular range. Additionally, certain reflections are compatible with the presence of orthoclase [(K$_{0.98}$Ba$_{0.02}$)(AlSi$_3$O$_8$)], identified from file PDF 01-083-6912. This phase, which also belongs to K-feldspars, presents peaks in regions close to those of microcline, making their discrimination difficult due to overlapping of their respective lines. The coexistence of plagioclase and K-feldspars therefore indicates a complex assemblage of quartz and feldspars.

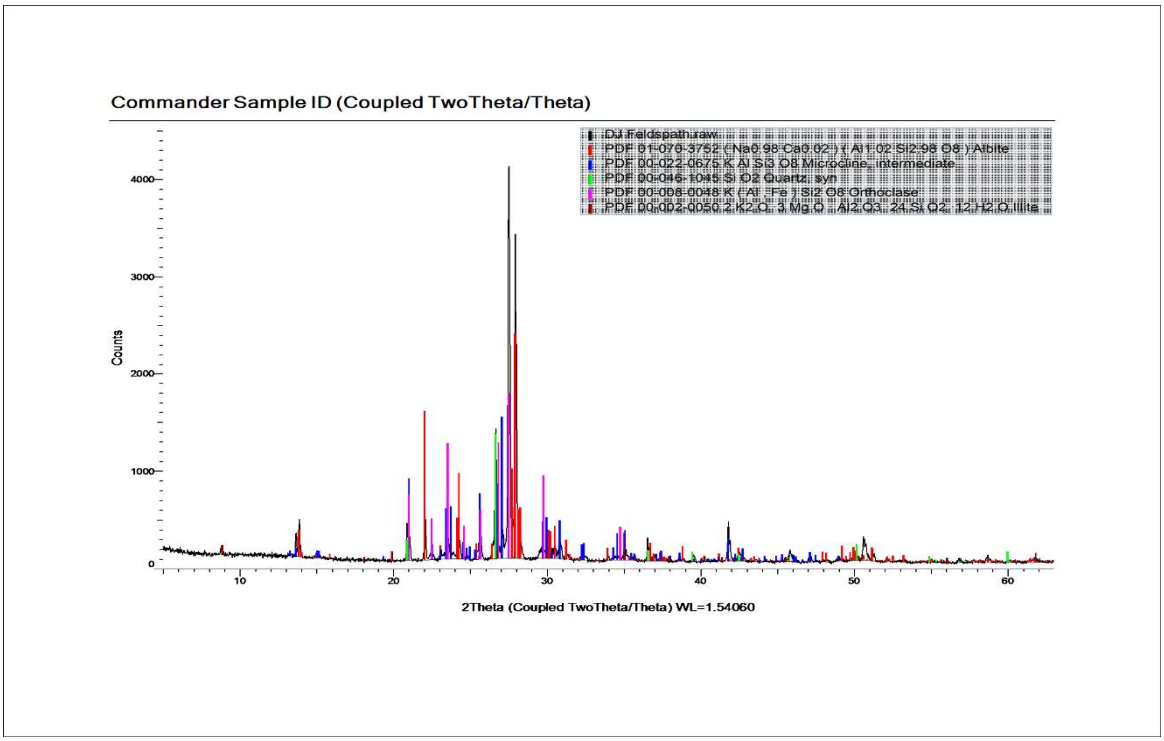

Figure 9:X-ray diffraction (XRD) spectrum of the Djombo sample, showing feldspar reflections.

The diffractogram also reveals the presence of subordinate phases of ferromagnesian and silicate nature (Fig. 10). Biotite-1M [$K(Mg,Fe^{2+})_3(Al,Fe^{3+})Si_3O_{10}(OH,F)_2$], identified from PDF file 00-042-1414, is suggested by several low-intensity reflections, particularly at low angles, around 8.5–9° (2θ), as well as in certain overlap zones with feldspars. This mica phase is present in minor proportions, but its presence indicates a significant ferromagnesian contribution to the mineral assemblage.

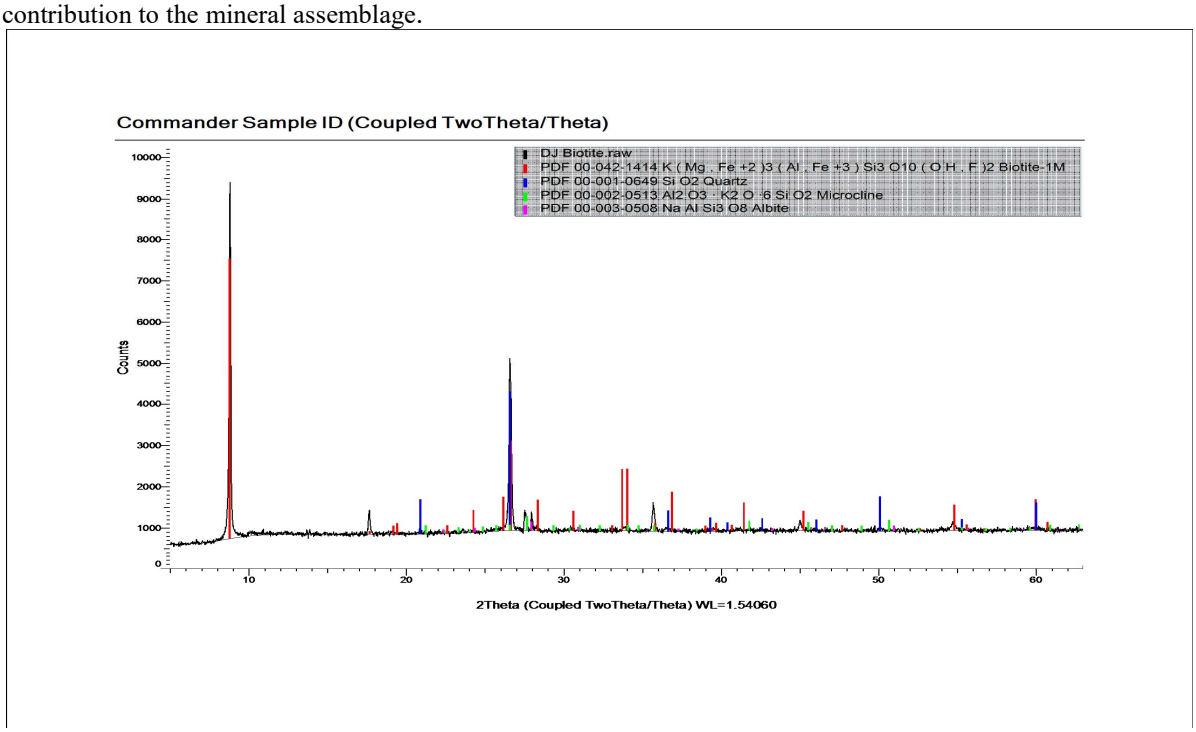

Figure 10:X-ray diffraction (XRD) spectrum of the Djombo sample, showing biotite reflections.

The mineralogical assemblage recorded in the Table is typical of a peraluminous granite that has undergone hydrothermal alteration in greenschist facies (Evans, 1982).

Table: Mineralogical composition of Djombo granite (DDJ)

Mineral	Chemical formula	PDF reference	Relative abundance
Quartz	SiO_2	01-079-1910	Dominant phase
Microcline (K-feldspar)	$KAlSi_3O_8$	00-019-0932	Second major phase
Albite (Na, Ca feldspar)	$(Na,Ca)Al(Si,Al)_3O_8$	00-041-1480	Second major phase
Biotite	$K(Mg,Fe^{2+})_3(Al,Fe^{3+})Si_3O_{10}(OH,F)_2$	00-042-1414	Subordinate phase
Trémolite	$Ca_2Mg_5Si_8O_{22}(OH)_2$	00-009-0437	Phase secondaire

Gleb pegmatite (Sample PGL I)

The X-ray diffraction pattern of sample PGL I, recorded in θ–2θ geometry under Cu Kα radiation (λ = 1.54060 Å), reveals a particularly simple mineralogical signature, dominated by a largely predominant crystalline phase (Fig. 11). The diffraction pattern is characterized by a limited number of reflections, all narrow, intense, and well-defined, on a very low diffuse background. The spectrum is dominated by a series of intense, sharp, and well-defined peaks, indicating a high degree of crystallinity of the analyzed mineral.

The main peak appears at an angle of 2θ ≈ 26.6°, with an intensity exceeding 11,000 counts, which is typical of primary quartz (SiO_2) diffraction. Other significant peaks are observed at 20.8°, 36.6°, 39.5°, 50.1°, and 59.9°, and are also characteristic of this mineral.

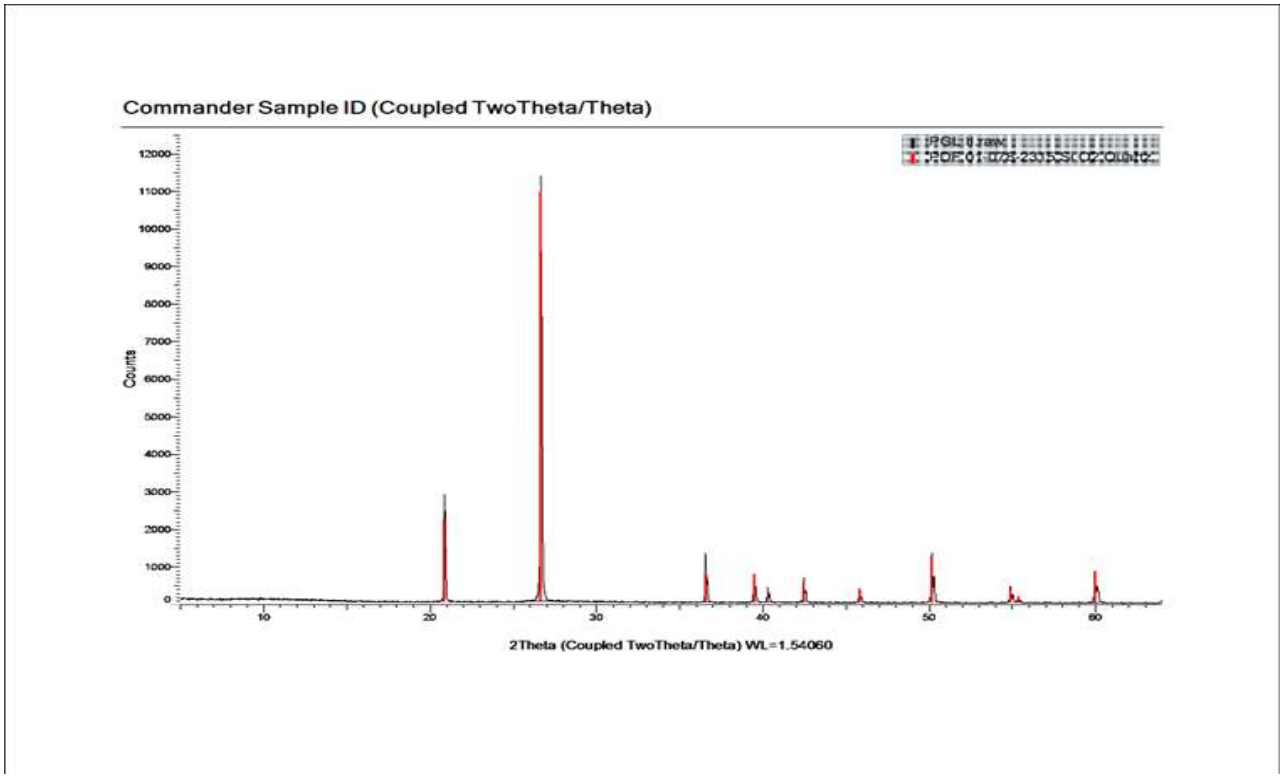

Figure 11:X-ray diffraction (XRD) spectrum of the pegmatite sample, showing quartz reflections.

Discussion:-

Petrogenesis and magmatic affinities of granitoids

Our results reveal two post-collisional magmatic facies: a peraluminous granite (Djombo) and a calc-alkaline granite (Gleb), whose mineralogical assemblage was precisely confirmed by XRD. These data corroborate the work of Isseini et *al.,* (2013) and Shellnutt et *al.,* (2017, 2020) on Ediacaran (~570-560 Ma) magmatism in central Chad. The originality of our approach lies in the microstructural demonstration of crystallization in a decompression context (crustal relaxation), favoring alkali feldspar exsolution and the appearance of primary muscovite.

Significance of tremolite and dynamics of the Saharan Metacraton

The formal identification by XRD of tremolite within an initially peraluminous granite constitutes a major particularity of this work. The presence of this amphibole indicates intense hydrothermal alteration (greenschist facies) by calcium- and magnesium-rich fluids. This observation fits perfectly with models of Saharan Metacraton destabilization (Abdelsalam et *al.,* 2002; Liégeois et *al.,* 2013). It demonstrates that the southern margin of the metacraton was not a rigid block, but a reactivated and fractured margin, acting as a drain for deep hydrothermal fluids during Pan-African post-orogenic relaxation.Synthesizing our results with regional data, we propose that the Batha Massif is located in a zone of major tectonic reactivation at the southern margin of the Saharan Metacraton, probably corresponding to the eastern extension of the heavy gravity anomaly identified by Louis (1970) and Braitenberg et *al.,* (2011). This structure, which crosses the Guéra Massif and separates Mayo-Kebbi from Ouaddaï, could represent a deep suture marking the boundary between the relict Chad craton to the north and more strongly reactivated domains to the south.

Structural evolution and metallogenic potential

Finally, analysis of Gleb veins reveals a single-phase signature of exceptionally pure quartz (>95% by XRD) coupled with spectacular cataclastic texture. This result proves the injection of siliceous fluids into active shear zones, corroborating classic models of orogenic gold (Sibson et *al.,* 1988; Goldfarb et *al.,* 2005). The unprecedented conjunction identified in this studyallanite-bearing fertile granites, greenschist facies alteration (tremolite), and brittle deformation (cataclasis) scientifically validates the strong gold potential of the Batha Massif and encourages mineral exploration along the lineaments of the Saharan Metacraton.

Conclusion:-

The different approaches used on the formations of the Djombo and Gleb mounts (Batha Massif) have clarified their petrographic nature, mineralogical composition, and geodynamic framework in the context of Pan-African orogenesis. Results reveal two post-collisional granitic facies: a peraluminous biotite-muscovite granite (Djombo) and a calc-alkaline amphibole-biotite granite enriched in allanite (Gleb), emplaced during crustal relaxation (~570-560 Ma) following the Saharan Metacraton – Congo Craton collision. XRD analysis confirms a typical quartz-feldspar-biotite assemblage and identifies tremolite for the first time, a mineral absent from previous Guéra studies. The presence of tremolite indicates intense hydrothermal alteration (greenschist facies) by Ca-Mg fluids, indicating that Batha is located in a zone of major tectonic reactivation at the southern margin of the Saharan Metacraton. This mineral constitutes a marker of the metacratonic heritage partially remobilized during Pan-African orogenesis. The Gleb pegmatite, composed of pure quartz (>95%) with cataclastic texture, represents the ultimate stage of this hydrothermal evolution. The association of fertile granites + tremolite + cataclastic quartz veins constitutes a signature favorable to orogenic gold deposits, validating the metallogenic potential of the Batha Massif and opening perspectives for regional exploration along Saharan Metacraton structures. Complementary studies (U-Pb geochronology, geochemistry, isotopes) would refine this model and better constrain the evolution of Batha within the framework of the Saharan Metacraton.

Acknowledgments:-

This work was carried out thanks to funding from the Romanian Ministry of Foreign Affairs, within the framework of a mobility organized by the Agence Universitaire de la Francophonie (AUF). We would like to thank the Geology Laboratory of Babeș-Bolyai University (Cluj-Napoca, Romania) for its hospitality during the analytical phase, with special mention to assistant Călin-Gabriel Tămaș and technician Sergiu Drăgușanu for their technical assistance.

References:-

1. **Abdelsalam, M.G., Liégeois, J.-P., Stern, R.J., 2002.** The Saharan Metacraton. Journal of African Earth Sciences 34, 119–136. https://doi.org/10.1016/S0899-5362(01)00063-4.

2. **Blades, M.L., Shellnutt, J.G., Reavy, R.J., Jahn, B.-M., 2021.** Age and hafnium isotopic evolution of zircons from the Guéra Massif, south-central Chad: Implications for the evolution of the Central African Orogenic Belt. Precambrian Research 357, 106148. https://doi.org/10.1016/j.precamres.2021.106148.
3. **Braitenberg, C., Mariani, P., Ebbing, J., Sprlak, M., 2011.** The enigmatic Chad lineament revisited with global gravity and gravity-gradient fields. In: Van Hinsbergen, D.J.J., Buiter, S.J.H., Torsvik, T.H., Gaina, C., Webb, S.J. (Eds.), The Formation and Evolution of Africa: A Synopsis of 3.8 Ga of Earth History. Geological Society, London, Special Publications 357, pp. 329–341. https://doi.org/10.1144/SP357.18.
4. **Barbarin, B., 1999.** A review of the relationships between granitoid types, their origins and their geodynamic environments. Lithos 46, 605–626. https://doi.org/10.1016/S0024-4937(98)00085-1.
5. **Chappell, B.W., White, A.J.R., 1974.** Two contrasting granite types. Pacific Geology 8, 173–174.
6. **Evans, B.W., 1982.** Amphiboles in metamorphosed ultramafic rocks. In: Veblen, D.R., Ribbe, P.H. (Eds.), Amphiboles: Petrology and Experimental Phase Relations. Reviews in Mineralogy 9B. Mineralogical Society of America, Washington, DC, pp. 98–113.
7. **Ferré, E.C., Deleris, J., Bouchez, J.L., Lar, A.U., Peucat, J.J., 2002.** The Pan-African reactivation of Eburnean and Archaean provinces in Nigeria: structural and isotopic data. Journal of the Geological Society, London 159, 83–95. https://doi.org/10.1144/0016-764901-055.
8. **Goldfarb, R.J., Baker, T., Dubé, B., Groves, D.I., Hart, C.J.R., Gosselin, P., 2005.** Distribution, character, and genesis of gold deposits in metamorphic terranes. In: Hedenquist, J.W., Thompson, J.F.H., Goldfarb, R.J., Richards, J.P. (Eds.), Economic Geology 100th Anniversary Volume. Society of Economic Geologists, Littleton, CO, pp. 407–450. https://doi.org/10.5382/AV100.14.
9. **Groves, D.I., Goldfarb, R.J., Gebre-Mariam, M., Hagemann, S.G., Robert, F., 1998.** Orogenic gold deposits: A proposed classification in the context of their crustal distribution and relationship to other gold deposit types. Ore Geology Reviews 13, 7–27. https://doi.org/10.1016/S0169-1368(97)00012-7.
10. **Isseini, M., André-Mayer, A.-S., Vanderhaeghe, O., Barbey, P., Deloule, E., 2013.** A-type granites from the Pan-African orogenic belt in south-western Chad constrained using geochemistry, Sr–Nd isotopes and U–Pb geochronology. Lithos 153, 39–52. https://doi.org/10.1016/j.lithos.2012.07.001.
11. **Kasser, M., 1995.** Carte géologique de la République du Tchad à 1/1 500 000. Bureau de Recherches Géologiques et Minières (BRGM), Orléans, France.
12. **Liégeois, J.-P., Abdelsalam, M.G., Ennih, N., Ouabadi, A., 2013.** Metacraton: Nature, genesis and behavior. Gondwana Research 23, 220–237. https://doi.org/10.1016/j.gr.2012.02.016.
13. **Louis, P., 1970.** Contribution géophysique à la connaissance géologique du bassin du lac Tchad. Mémoires ORSTOM 42. Office de la Recherche Scientifique et Technique Outre-Mer (ORSTOM), Paris, France, 311 p.
14. **Penaye, J., Toteu, S.F., Van Schmus, W.R., Nzenti, J.P., 2006.** U–Pb and Sm–Nd preliminary geochronologic data on the Yaoundé series, Cameroon: Re-interpretation of the Neoproterozoic rocks as the suture zone between the Congo craton and the Adamawa–Yadé domain. Journal of African Earth Sciences 44, 473–486. https://doi.org/10.1016/j.jafrearsci.2005.11.014.
15. **Tchameni, R., Mezger, K., Nsifa, N.E., Pouclet, A., 2013.** Crustal origin of Early Proterozoic syenites in the Congo Craton (Ntem Complex), South Cameroon. Lithos 57, 23–42. https://doi.org/10.1016/S0024-4937(00)00072-4.
16. **Robert, F., Poulsen, K.H., 2001.** Vein formation and deformation in greenstone gold deposits. In: Richards, J.P., Tosdal, R.M. (Eds.), Structural Controls on Ore Genesis. Reviews in Economic Geology 14. Society of Economic Geologists, Littleton, CO, pp. 111–155.
17. **Sobh, M., Ebbing, J., Mansi, A.H., Götze, H.-J., 2020.** Inverse and 3D forward gravity modelling for the estimation of the crustal thickness of Egypt. Tectonophysics 752, 52–68. https://doi.org/10.1016/j.tecto.2018.12.002.
18. **Shellnutt, J.G., Reavy, R.J., Viscaíno, C., Kalsbeek, F., Jahn, B.-M., 2017.** The Ediacaran felsic rocks of the Guéra Massif, south-central Chad: Evidence for the northward continuation of the Neoproterozoic orogen. Precambrian Research 301, 172–190. https://doi.org/10.1016/j.precamres.2017.09.008.
19. **Shellnutt, J.G., Reavy, R.J., Yeh, M.-W., Lee, T.-Y., Iizuka, Y., 2020.** The origin of Late Ediacaran post-collisional granites near the Chad Lineament, Saharan Metacraton, south-central Chad. Lithos 376–377, 105780. https://doi.org/10.1016/j.lithos.2020.105780.
20. **Sibson, R.H., Robert, F., Poulsen, K.H., 1988.** High-angle reverse faults, fluid-pressure cycling, and mesothermal gold-quartz deposits. Geology 16, 551–555. https://doi.org/10.1130/0091-7613(1988)016.
21. **Vincent, P.M., 1956.** Carte géologique de reconnaissance du Tchad (feuilles de Mongo, Melfi, Abou Déïa, Am Timan). Service des Mines, Gouvernement Général de l'Afrique Équatoriale Française (A.E.F.), Brazzaville, Congo.